

IMPERFECTION SENSITIVITY OF THIN PLATES LOADED IN SHEAR

FRANC SINUR¹, PRIMOŽ MOŽE¹, KLEMEN REJEC²,
GAŠPER LUŽAR³, DARKO BEG¹

Abstract. The paper deals with imperfection sensitivity analysis of longitudinally stiffened thin plates loaded in shear. The aim of this paper is to demonstrate the use of optimization method for direct determination of the worst imperfection shape. New linear constraints are considered in optimization method in order to find not only the worst but also realistic imperfection shape. Further on, different solutions of arbitrary shapes that are used to estimate the worst imperfection are introduced and compared. Finally, a parametric analysis seeking the worst imperfection shape is performed and discussed.

Key words: plate buckling, worst initial imperfections, longitudinal stiffeners, sensitivity analysis, GMNIA.

1. INTRODUCTION

The increased capacity of computers and the possibilities of numerical tools available today facilitate the use of advanced calculation models in everyday design practice. Thus, in design of structures the use of material and geometrical nonlinear analysis considering imperfections to design structures is growing. Such analysis allows a detailed insight in the behaviour of structures or structural elements. The design approach, however, requires a lot of experience in order to build a convenient and proper numerical model and to interpret the results correctly. The initial boundary conditions, constitutive material laws and initial imperfections have an important influence on the behaviour and resistance of the structure or structural element under consideration. At the University of Ljubljana, Chair for Metal Structures, an advanced optimization method for direct determination of the most unfavourable imperfection of the structural element was developed [1, 2]. This optimization method, based on direct and sensitivity analysis and optimization algorithms, was implemented on thin plates subjected to shear stresses. The

¹ University of Ljubljana, Faculty of Civil and Geodetic Engineering, Slovenia

² University of Ljubljana, Faculty of Civil and Geodetic Engineering, Slovenia

³ Bürogemeinschaft Kuhlmann Gerold Günther Eisele, Germany

optimization function is determined as the minimum value of the load proportional factor (LPF), which is a function of the imperfection shapes (buckling modes, Fourier terms, etc.), and it presents the worst imperfection shape for the structure.

The paper presents an extended study, which deals with the search for the most unfavourable imperfection shape for representative slender plates (stiffened plates) subjected to pure shear. The constraints of the optimization process were determined by the maximum allowable imperfection amplitude obtained from the production tolerances and design rules for plated structural elements [3–5] and by the maximum curvature of the imperfect geometry. Special attention was devoted to the constraint of the maximum curvature.

2. METHODOLOGY FOR THE DETERMINATION OF THE MOST UNFAVOURABLE IMPERFECTION

Initial imperfections are the consequence of the production process and cannot be avoided. When dealing with slender elements, i.e. thin plates subjected to compressive stresses, the results of geometrical material nonlinear analysis considering imperfections strongly depend on the imperfection shape and its amplitude. Thus, it is important to consider the most unfavourable actually possible imperfection shape, which will lead to safe and reliable assessment of the resistance of the analysed structural element.

A computationally less expensive optimization method that retains the generality of the optimization based “definitely worst” imperfection approach was developed by Kristanič and Korelc [1, 2, 6]. The basic idea of the approach is to replace the nonlinear optimization problem with an iterative procedure that involves only linear optimization problems. Within the iteration the objective function for the minimum ultimate load is constructed by means of a fully nonlinear direct and first order sensitivity analysis. Constraints on the shape and the amplitude of the imperfections are taken into account. When carefully constructed, they remain linear, therefore enabling the use of efficient and readily available linear programming algorithms for obtaining the solution of the corresponding optimization problem.

2.1. REPRESENTATION OF IMPERFECTIONS

The applied initial imperfection shape with specified amplitudes has to represent a change in the geometry of a structure in the most unfavourable way so that the ultimate load of the imperfect structure is as small as possible. The imperfections are represented as a linear combination of the chosen basic shapes within maximum out-of-plane amplitude e_0 prescribed by the principle of equivalent geometrical imperfections. Equivalent geometrical imperfections include geometrical

and structural imperfections. Geometrical imperfections can be augmented to include structural imperfections that are not included directly into the finite element model. Structural imperfections arise from the manufacturing method; e.g. residual stresses produced by welding. The geometry of an imperfect structure \mathbf{X} is defined by:

$$\mathbf{X} = \mathbf{X}_p + \sum_{j=1}^N \alpha_j \mathbf{\Gamma}_j, \quad (1)$$

where \mathbf{X}_p is the initial perfect geometry, α_j are the unknown shape parameters and $\mathbf{\Gamma}_j$ are the base shapes. The unknown shape parameters α_j are obtained as the solution of the optimization problem. The base shapes can be chosen arbitrarily, but they have to be linearly independent in order to have a well-defined minimum of the corresponding optimization problem. The overall numerical efficiency of the procedure strongly depends on the number of the base shapes (N).

2.2. DESCRIPTION OF THE ALGORITHM

In the presented approach a fully geometrically and materially nonlinear analysis is used. When dealing with thin-walled structures with moderate thickness, it is necessary to take into account geometrical and material nonlinearity. Since the algorithm starts from the beginning with imperfect structure, bifurcation points usually do not occur prior reaching the limit point in the load-deformation curve.

Within this method the most unfavourable initial imperfection shape is sought, defined by shape base $\mathbf{\Gamma}$ and shape parameters α at which the ultimate load will be the lowest [1]. Unknown shape parameters α are evaluated iteratively by an optimization process. The iterative procedure for the k^{th} step can be written as:

$$\begin{aligned} \mathbf{X}_k &= \mathbf{X}_{k-1} + \Delta\mathbf{X}_k \\ \Delta\mathbf{X}_k &= \sum_{i=1}^N \Delta\alpha_i^k \mathbf{\Gamma}_i \\ \alpha_i^k &= \alpha_i^{k-1} + \Delta\alpha_i^k, \\ \bar{\mathbf{X}}_k &= \sum_{i=1}^N \Delta\alpha_i^k \mathbf{\Gamma}_i \end{aligned} \quad (2)$$

where \mathbf{X}_k is the imperfect geometry, $\Delta\alpha_i^k$ the increment of the imperfection parameters, $\Delta\mathbf{X}_k$ the increment of the imperfection and $\bar{\mathbf{X}}_k$ the total imperfection. The increment of the imperfection parameters in the k^{th} iteration $\Delta\alpha_i^k$ is obtained as a solution of the corresponding optimization problem [1, 2]. The flowchart of the method is illustrated in Fig. 1. The algorithm starts with the first base shape $\mathbf{\Gamma}_1$, normalized by amplitude e_0 , as the initial guess \mathbf{X}_0 for the geometry of the imperfect structure:

$$\alpha_i^0 = 0; \Delta\alpha_i^0 = \begin{cases} \frac{e_0}{\max \Gamma_i} & i = 1 \\ 0 & i \neq 1 \end{cases} \quad (3)$$

$$\mathbf{X}_0 = \mathbf{X}_p + \Delta\alpha_1^0 \Gamma_1$$

and then improves the solution by solving a sequence of optimization problems until the convergence condition $\|\Delta\alpha_i^k\| < tolerance$ is reached. Within each step of the iterative procedure a fully nonlinear direct and sensitivity analysis of the structure with imperfect geometry \mathbf{X}_k is performed, followed by the formulation and solution of the optimization problem.

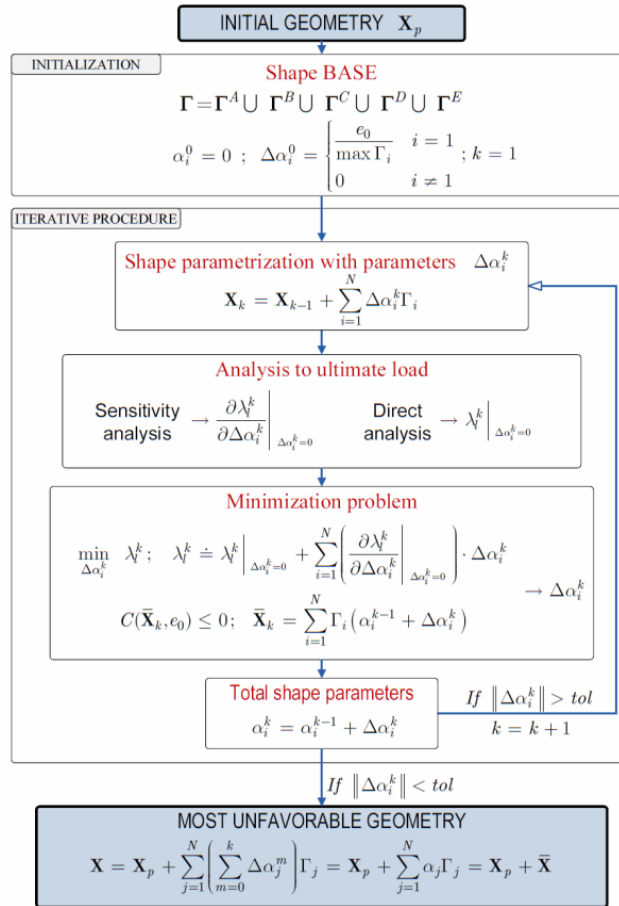


Fig. 1 – Flowchart of the method for the determination of the most unfavourable imperfection [1].

2.3. SHAPE BASE

The shape base is used to find the most unfavourable initial imperfection. The obvious choice are the buckling modes of the structure obtained by the initial buckling analysis. Alternative and cheaper to evaluate are the eigenvectors of initial elastic tangent matrix. Other possible shapes are deformation shapes of the structure in elastic and plastic range and arbitrarily defined shapes. In this work only the arbitrarily defined shapes were used.

2.4. ARBITRARILY DEFINED SHAPES

Shape base defined in terms of fourier series

The base shapes were defined as two-dimensional sine functions in order to keep all edges straight, without any imperfection. The only parameter that defines the considered shapes is the number of terms of Fourier series that was considered. The shapes were defined as:

$$\mathcal{S}_1 \times \mathcal{S}_2 = \{s_1 \cdot s_2; s_1 \in \mathcal{S}_1, s_2 \in \mathcal{S}_2\}, \quad (4)$$

$$\mathcal{S}_1 = \left\{ \sin\left(\frac{i\pi x}{A}\right) \right\}; i=1, 2, \dots, n, \quad (5)$$

$$\mathcal{S}_2 = \left\{ \sin\left(\frac{i\pi y}{B}\right) \right\}; i=1, 2, \dots, m, \quad (6)$$

where A and B represent the length and the width of the analysed plate, n defines the number of half sine waves in x and m in y direction, respectively. The number of shape base Γ is equal to product $n \times m$. The base shapes defined according to expression (4) for $n = m = 3$ are illustrated in Fig. 2.

Specially defined base shapes

Another type of base shapes called specially defined shapes were considered in the analysis. The shapes were defined with sine function, where one half wave is assumed in transverse direction and n waves in longitudinal direction. The number of shapes in transverse direction depends on the number of longitudinal stiffeners, e.g. for two longitudinal stiffeners the possible number of shapes is $6 \times n$, where 6 corresponds to 6 possible shapes in transverse direction, as presented in Fig. 3. For shape no. 1 the length of the half sine wave is equal to the width of plate B . Shapes no. 2 and 3 correspond to wave length $2 \times B/3$ (as the stiffeners are equally spaced); it means that the wave is stretched over two subpanels with the maximum amplitude located at the position of the longitudinal stiffener. For the last 3 shapes, shapes no. 4, 5 and 6, the shape is defined with wave length $B/3$ and is positioned over one subpanel, while the other subpanels remain straight.

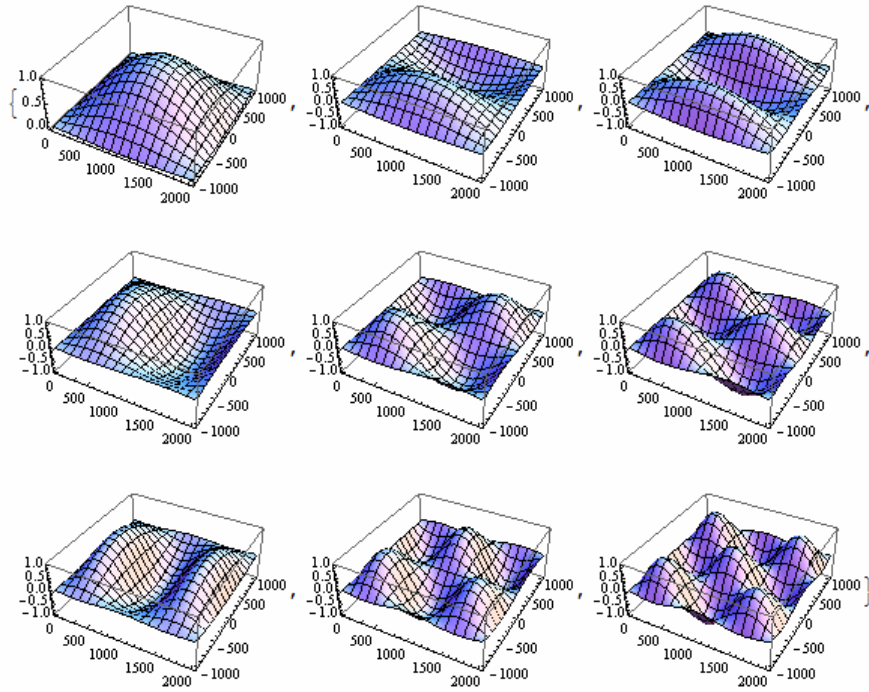


Fig. 2 – Base shapes for $m = n = 3$.

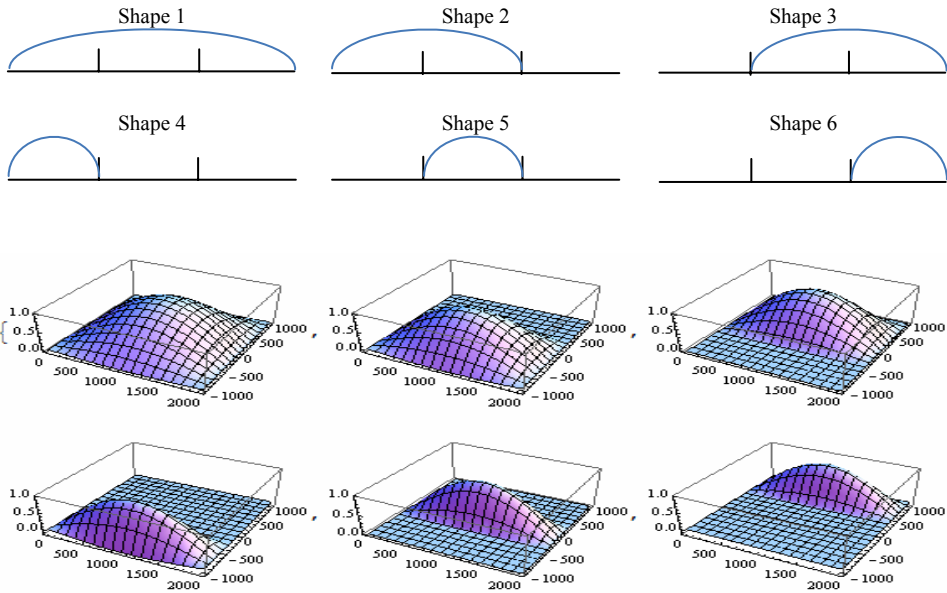


Fig. 3 – Specially defined shapes for $n = 1$.

2.5. NUMERICAL MODEL

The numerical model consists of simply supported plate, longitudinal stiffeners and three stiff bands (Fig. 4). The boundary conditions were as follows: all four edges were simply supported; the left edge was restrained also in the longitudinal direction. The vertical supports in the other three edges were defined in nodes between base plate and stiff band. Additional stiff band was modeled in edges in order to simulate the same conditions as in the left edge, to keep the edge undeformed in its longitudinal direction. The load was applied as shear line load along edges, as presented in Fig. 4. The amplitude of the load was set to plastic shear resistance of the plate.

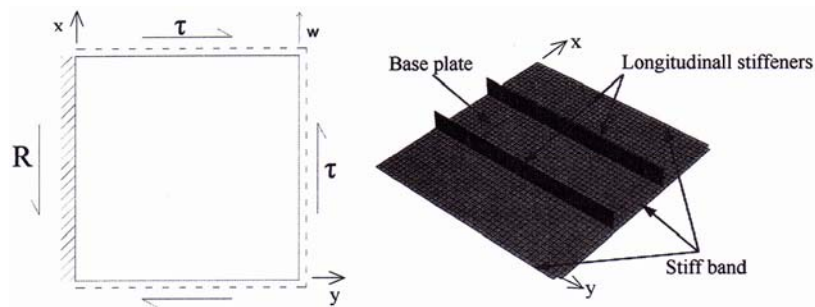


Fig. 4 – Numerical model – boundary conditions and load application.

3. LINEAR CONSTRAINTS

By using optimization approach to find the most unfavourable imperfection shape, the linear constraints in terms of maximum imperfection amplitude have to be defined. Another parameter which significantly influences the solution for the most unfavourable imperfection is, as already mentioned, the maximum curvature. These two parameters were the key terms that influenced the solution for the most unfavourable imperfection shape defined by using optimization approach.

When numerical tools are used to design a structure, in most cases equivalent geometric imperfections are used. They take into account both geometric as well as structural imperfection (residual stresses) by increased amplitude of geometric imperfection. Annex C of EN 1993-1-5 provides recommendations on possible types of initial imperfection shapes and amplitudes that should be accounted for in FEM design of thin plated structural elements.

The amplitudes of the imperfections were limited according to the EN 1993-1-5 specifications, while the influence of the curvature limit was studied within the study presented in this paper, and based on it the maximum allowed curvature was defined.

It has already been demonstrated [1, 7] that out-of-plane displacement constraint only might lead to initial imperfections that are unrealistic and consequently very

conservative due to high reduction of the ultimate resistance. Thus, an additional constraint, such as maximum curvature, should be considered in the optimization process. Sensitivity analysis was performed in order to establish the influence of the curvature amplitude on the behaviour and the resistance of the plate subjected to in-plane stresses and to define the constraints for parametric study.

In Table 1 the maximum amplitudes for global and local imperfections taken from EN 1993-1-5 (Annex C) are given, where n_{st} corresponds to the number of longitudinal stiffeners. The maximum amplitude of the imperfection is defined as:

$$e_0 = e_G + 0.7e_L, \quad (7)$$

with global imperfection e_G as the leading and local e_L as the accompanying imperfection. The simplest function which was used to generate initial imperfection was sine function with the maximum out-of-plane amplitude and consequently also the maximum curvature at the mid span. For this imperfection shape the curvature is very small and could be too strict for real cases. A series of extra functions was defined; they are similar to sine function with maximum amplitude shifted to $x_{max} = 2/5A$, $1/3A$ and $1/4A$, where A is the panel length. These functions were defined to get different values of the curvature, while the maximum out-of-plane amplitude remained the same. The functions were defined as a 4th order polynomial:

$$f(x) = ax^4 + bx^3 + cx^2 + dx + e. \quad (8)$$

Table 1
Maximum imperfection amplitudes defined in EN 1993-1-5

Global imperfection amplitude e_G	$\min \left\{ \frac{A}{400}, \frac{B}{400} \right\}$
Local imperfection amplitude e_L	$\min \left\{ \frac{A}{200}, \frac{B}{(n_{st} + 1) \cdot 200} \right\}$

Coefficients a , b , c , d and e were defined to fulfil the following conditions: $f(0) = 0$, $f(x = a) = 0$, $f(x = x_{max}) = e_{max}$, $f'(x = x_{max}) = 0$ and $f'(x = a) = -\pi/a$. The last condition arises from the first derivation if sine function is evaluated at $x = A$.

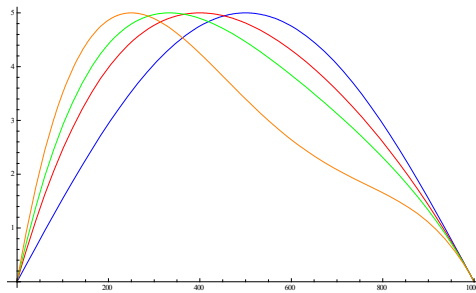


Fig. 5 – 4th order polynomials with maximum at 1/4, 1/3, 2/5 and 1/2 of the span.

It is obvious that the maximum curvature will be obtained for the curve with the largest shift of the maximum amplitude position, i.e. at $x = A/4$ (Fig. 5). The upper bound for the maximum curvature is defined with the curvature obtained for elastic bending moment, when the first fibre starts to yield. This value is constant for all lengths of the plate and depends solely on the plate thickness t :

$$\kappa_{yield} = \frac{2\varepsilon_y}{t}. \quad (9)$$

In Fig. 6 the maximum curvature for the selected 4th order functions and the upper bound curvature for three different plate thicknesses are plotted ($t = 10$ mm, 20 mm and 30 mm). The maximum curvature among the given functions is found for the one with maximum amplitude at $x = A/4$, which is also evident from Fig. 5. The upper bound κ_{yield} depends only on the plate's thickness; therefore, the curvature does not change due to the change of the panel size. For a plate with thickness $t = 20$ mm, κ_{yield} is smaller than the curvature obtained with function with maximum at $x = A/4$, when panel length is less than $A = 600$ mm. Therefore, up to this point the maximum curvature is limited with the upper bound limit κ_{yield} and from this point forward the limit is defined from maximum curvature that is defined with function with maximum at $x = a/4$.

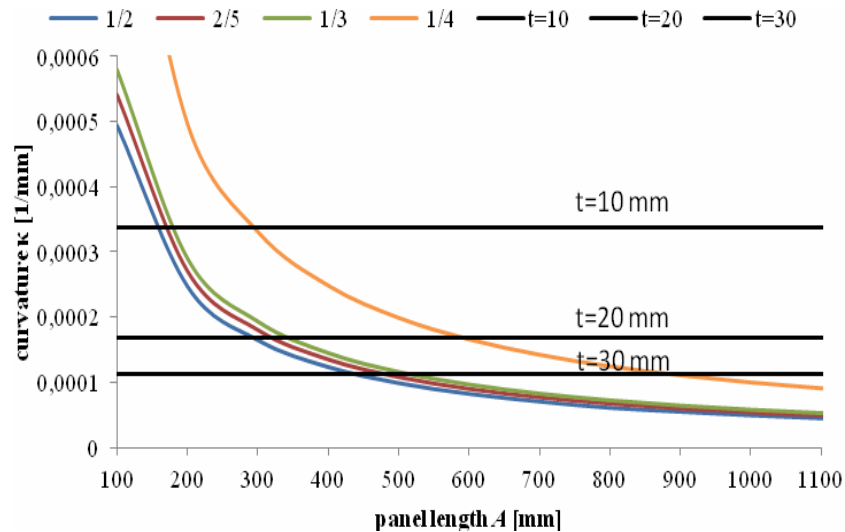


Fig. 6 – Curvature as a function of panel length a [mm].

The influence of the curvature amplitude on the most unfavourable imperfection shape solution and consequently on LPF for longitudinally stiffened plate (two cases: one and two longitudinal stiffeners) subjected to pure shear is gathered in Table 2. By increasing the maximum allowed curvature the resistance of the plate drops, especially when the maximum curvature is increased from the

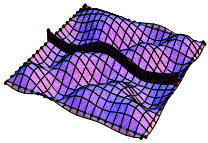
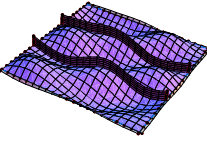
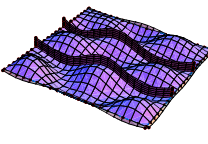
curvature of the function with maximum at $x = A/4$ to κ_{yield} and $2\kappa_{\text{yield}}$. Further on, the imperfection shape is very smooth for stricter curvature limit and vice versa, the imperfection shape becomes very rough when the curvature limit is set higher. This is a good reason why the maximum curvature should also be applied; it influences the imperfection shape in a way for it to become more realistic. For the studied cases a curvature limit defined with a function with maximum at $x = A/4$ is found to be a reasonable limit for the constraint because:

- The obtained imperfection shape is smooth.
- The resistance drop induced by higher curvature limits is too large and results in excessively conservative values of LPF.

The most unfavourable imperfection shape given in Table 2 proves that free edges of the numerical model are not straight. This is due to the fact, that the last line of the elements represents stiff band. The plate is straight where the stiff band is connected to the base plate which can also be identified from the figures below.

Table 2

Comparison of the most unfavourable imperfection shapes for different curvature constraints

		$f(x=a/4)=e_{\text{max}}$	$1 \times \kappa_{\text{Yield}}$	$2 \times \kappa_{\text{Yield}}$
1 stiffener	max. curvature [1/mm]	0.000155	0.000338	0.000676
	LPF	0.844	0.790	0.766
	Most unfavourable imperfection			
2 stiffeners	max. curvature [1/mm]	0.000161	0.000338	0.000676
	LPF	0.877	0.837	0.828
	Most unfavourable imperfection			

4. NUMERICAL ANALYSIS – REQUIRED NUMBER OF BASE SHAPES

The most unfavourable imperfection was sought for plates stiffened with one, two and four longitudinal stiffeners (Fig. 7). The material was modelled as bilinear without any strain hardening. The yield strength was set to $f_y = 355$ MPa, elastic modulus to $E = 210\,000$ MPa and Poisson's ratio to $\nu = 0.3$.

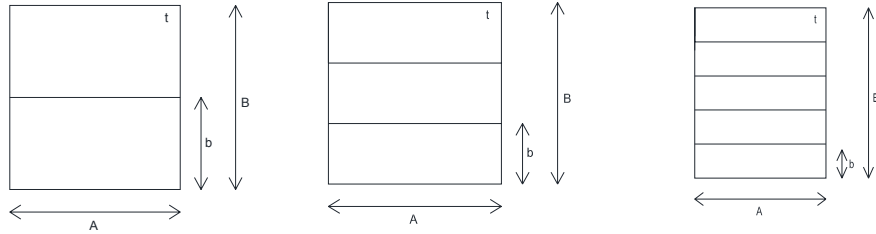


Fig. 7 – Geometry and dimension notations of studied stiffened plates.

First, the sensitivity analysis to determine the required number of base shapes and to define the mesh density was performed. This analysis was done for all three configurations of the plate (1, 2 and 4 stiffeners) with panel aspect ratio $\alpha = 1$, global panel slenderness $B/t = 200$ and normalized flexural stiffness of stiffener $\gamma = I_{sl}/I_p = 16.4$, where I_{sl} is the flexural stiffness of the stiffener taking into account the effective width of the plate and I_p is the flexural stiffness of the plate itself.

4.1. MESH DENSITY

Sensitivity analysis was performed for four different mesh densities: M10, M20, M40 and M80. The number corresponds to the number of elements used along the plate's length A . In Fig. 8 the influence of mesh density on the LPF factor is shown. Each curve corresponds to one of the plate's configurations. On y -axis the LPF factor obtained is normalized to the LPF factor obtained for mesh density M10, while on x -axis the mesh density is plotted. The mesh density M40 was found to be appropriate for further parametric study as no significant drop of LPF was obtained with a more dense mesh.

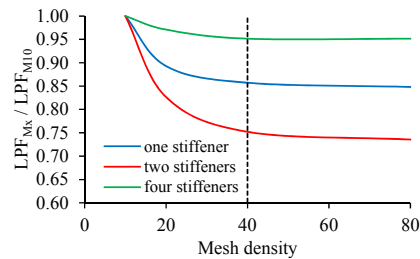


Fig. 8 – The influence of mesh density on LPF.

4.2. MINIMUM NUMBER OF BASE SHAPES

As the computational time significantly increases with the growing number of base shapes, the minimum number of base shapes that gives a sufficiently

reliable and accurate solution needs to be defined. The analysis was performed for base shapes defined in terms of Fourier series and for specially defined base shapes presented in Chapter 2.

The influence of the number of base shapes considered in the analysis is for plate with one and four longitudinal stiffeners shown in Fig. 9. The minimum required number of base shapes depends on the number of longitudinal stiffeners. Fewer shapes are needed for a plate with one stiffener than for a plate with four stiffeners. The results are presented for both forms of initial shapes; defined as Fourier terms and specially defined shapes. In Fig. 9 the legend notations $NFouRed = x$ describe how many terms of Fourier series are considered. For instance, $NFouRed = 4$ means that the first 4 terms of Fourier series are used to define base shapes as described in Chapter 2. This results in $4^2 = 16$ shapes. Similarly, label $NGlobObl = x$ provides information on the number of specially defined shapes in the longitudinal direction. The shapes in transverse direction are defined in Chapter 2 and depend on the number of longitudinal stiffeners (3 for one stiffener, 6 for two stiffeners and 15 for four stiffeners). $NGlobObl = 4$ means that in longitudinal direction functions with 1, 2, 3 and 4 half waves were considered and therefore for a plate with four longitudinal stiffeners $4 \times 15 = 60$ base shapes are obtained.

For a plate stiffened with one longitudinal stiffener at least 16 base shapes ($NFouRed = 4$) are required to get a reliable and accurate solution, which does not change significantly if higher terms of Fourier series are used. For specially defined shapes the minimum required number of base shapes is 9 ($NGlobObl = 3$). As already mentioned, a higher number of base shapes is required for plates with larger number of longitudinal stiffeners. This is especially evident when special types of base shapes are used. For 4 stiffeners the minimum number of shapes that has to be considered is 45 ($NGlobObl = 3$), whereas only 16 ($NFouRed = 4$) shapes are needed if the shapes are defined by using combinations of Fourier terms. If, however, more than 50 base shapes were considered, problems with convergence occurred in the analysis.

Based on the presented sensitivity analysis, the minimum number of base shapes was defined for the following parametric study. The most unfavourable imperfection shape was sought by using base shapes defined as Fourier terms (16 shapes considered, $NFouRed = 4$), and specially defined shapes ($3 \cdot \sum_{i=1}^{n_{st}} i$ considered shapes, where n_{st} is the number of longitudinal stiffeners, $NGlobObl = 3$).

The most unfavourable imperfection shape for plate with 4 longitudinal stiffeners is shown in Fig. 10. Increased number of shapes considered ($NFouRed = 8$ and $NGlobObl = 4$) does not produce any different imperfection shape than that obtained with $NFouRed = 4$ and $NGlobObl = 3$.

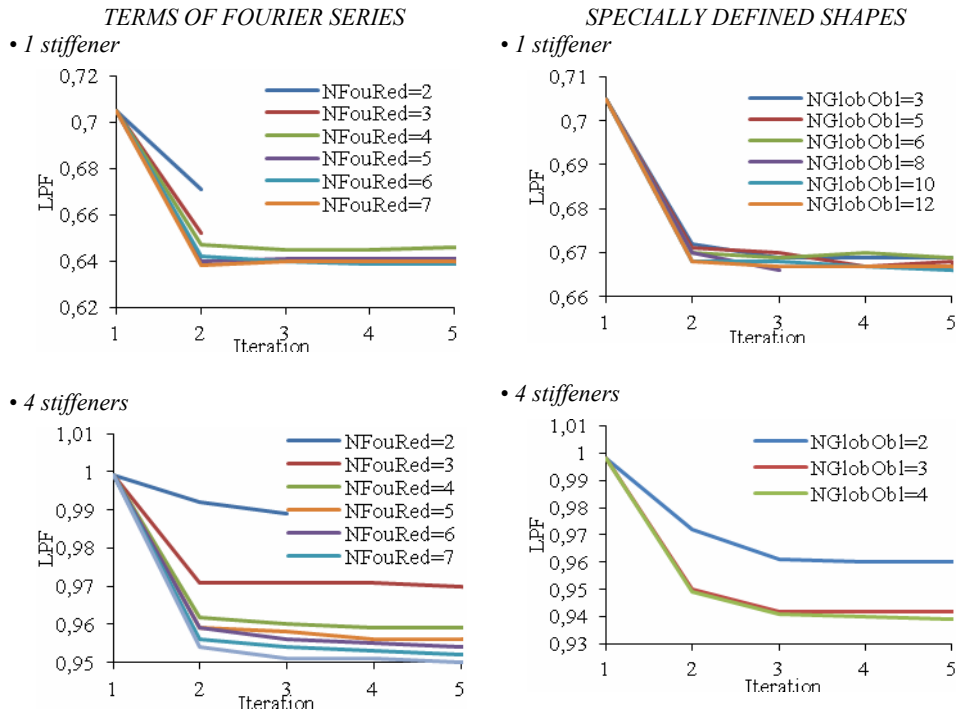
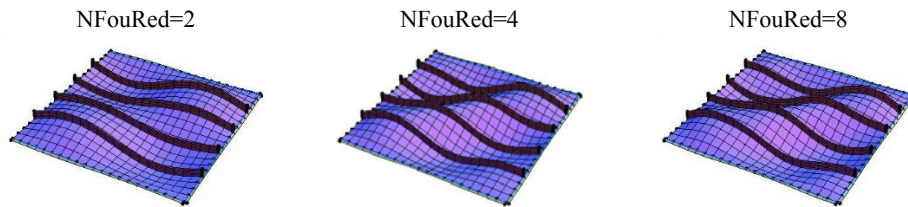


Fig. 9 – LPF factor obtained with different number of base shapes included in analysis.

Imperfection shapes defined with Fourier Terms



Imperfection shapes defined with specially defined shapes

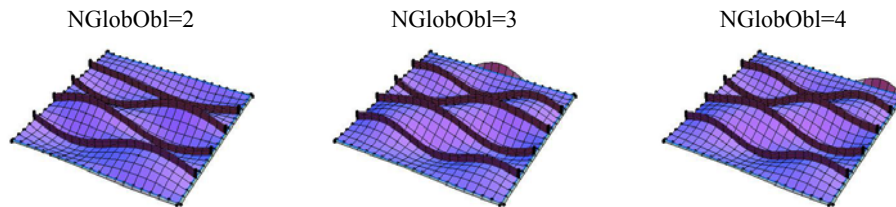


Fig. 10 – The most unfavourable imperfection shapes obtained with different numbers of base shapes considered.

4.3. PARAMETRIC STUDY

A parametric study was performed to determine the influence of the plate's slenderness and the stiffness of longitudinal stiffeners on the most unfavourable imperfection shape. The varied parameters within were:

- Number of longitudinal stiffeners $n = 1, 2, 4$.
- Slenderness of subpanel $b/t = 35, 50, 75, 100$.
- Stiffness of longitudinal stiffeners $\gamma = 18, 35, 110$.

Three different stiffnesses of longitudinal stiffener were studied. The stiffener with stiffness $\gamma = 35$ ensures that elastic global buckling of the subpanel is equal to elastic global buckling of the entire stiffened panel. In all cases the initial imperfection shape Γ_1 was defined as a combination of global Γ_G and local Γ_L imperfection shape as recommended in EN 1993-1-5.

In Fig. 11 the results obtained for plate stiffened with one stiffener and subpanel slenderness $b/t = 75$ are presented. The main results that were obtained and will be discussed are the initial imperfection and the final deformation shape as well as the LPF. The initial imperfections are compared to the deformed shape obtained at maximum LPF.

For all defined most unfavourable imperfection shapes that were calculated using shapes based on Fourier terms and also on specially defined shapes the LPF was always smaller compared to the LPF calculated with imperfections determined according to the EN 1993-1-5 recommendations (combination of global and local imperfections $\Gamma_G + 0.7 \Gamma_L$). Smaller LPF was found for imperfection shapes defined with Fourier terms. The imperfection shape defined with Fourier terms is smoother and very similar to the final deformation shape. Three buckling waves with orientation in the direction of tension field formation characterize the worst imperfection shape found with base shapes based on Fourier terms.

The difference of this LPF compared to the LPF obtained with the EN 1993-1-5 imperfection shape is much smaller if the worst imperfection shape is calculated with specially defined shapes. The imperfection shapes obtained are much more diverse with several waves. Tendency to global deformation shape was observed meaning that the imperfection shape approaches to the deformation shape if pool of specially defined shapes is increased. However, the number of the base shapes considered in this case was not high enough to get similar worst imperfection shape as with Fourier terms.

The results for plate stiffened with two longitudinal stiffeners and subpanel slenderness $b/t = 50$ are shown in Fig. 12. Also in this case the worst imperfection shape found is similar to the deformation shape. In contrast with the previous case, the similarity between the imperfection shape and the deformation shape is found also for the solution based on specially defined shapes. The LPF factor is, in comparison to the LPF obtained with the EN 1993-1-5 imperfections (values in brackets) in all cases smaller, where the difference varies from 3.6% to 6.9%. The results again prove that the worst imperfection shape is similar to the deformation shape. Similar conclusions were observed also for other parameters that were analysed within the parametric study.

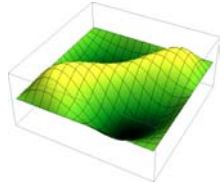
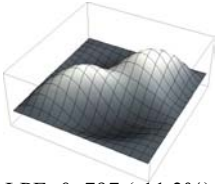
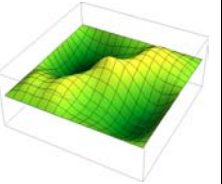
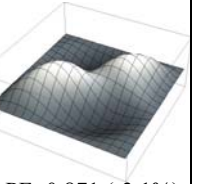
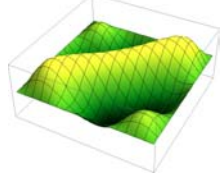
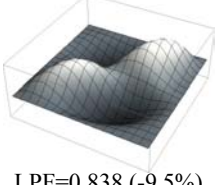
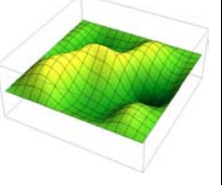
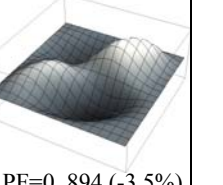
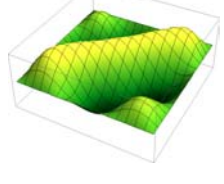
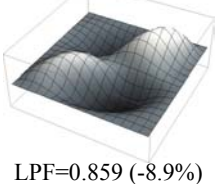
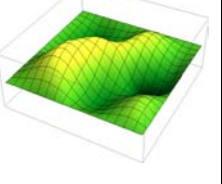
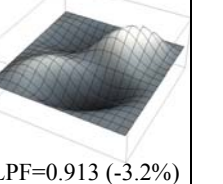
γ	Shapes based on Fourier terms		Specially defined shapes	
	Imperfection shape	Deformation shape	Imperfection shape	Deformation shape
18		 LPF=0.797 (-11.3%)		 LPF=0.871 (-3.1%)
35		 LPF=0.838 (-9.5%)		 LPF=0.894 (-3.5%)
110		 LPF=0.859 (-8.9%)		 LPF=0.913 (-3.2%)

Fig. 11 – Comparison of the most unfavourable imperfection and deformed shape for plate stiffened with one stiffener, $b/t = 75$.

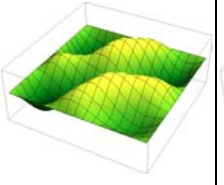
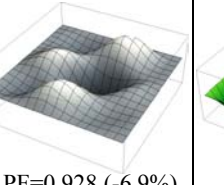
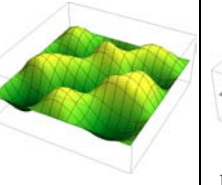
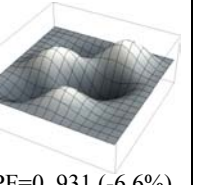
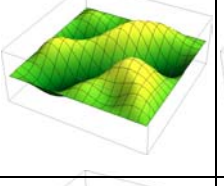
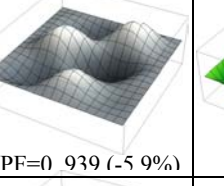
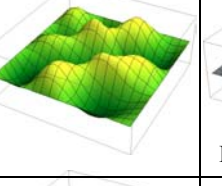
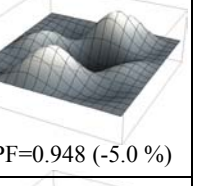
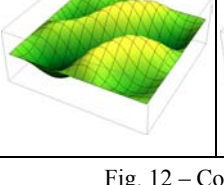
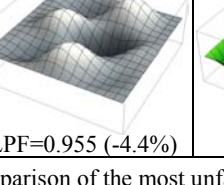
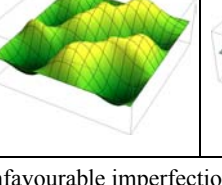
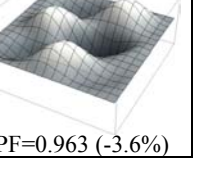
γ	Shapes based on Fourier terms		Specially defined shapes	
	Imperfection shape	Deformation shape	Imperfection shape	Deformation shape
28		 LPF=0.928 (-6.9%)		 LPF=0.931 (-6.6%)
55		 LPF=0.939 (-5.9%)		 LPF=0.948 (-5.0%)
165		 LPF=0.955 (-4.4%)		 LPF=0.963 (-3.6%)

Fig. 12 – Comparison of the most unfavourable imperfection and deformed shape for plate stiffened with two stiffeners, $b/t = 50$.

5. CONCLUDING REMARKS

The worst imperfection shape to obtain minimum resistance can be defined as superposition of different shapes. With the performed study we tried to answer the following questions:

- how the arbitrary shapes should be defined in order to get consistent and reliable results,
- how to find, next to maximum out-of-plane displacement, an additional linear constraint that will provide more realistic imperfection shapes and
- is there a simple way to define the worst imperfection shape?

It has been shown that the imperfection shape defined as a superposition of Fourier terms results in imperfection shapes with the lowest LPF and that the worst imperfection shape is smooth and similar to the deformed shape. The imperfection shape estimated with specially defined shapes gives a higher value of LPF and the corresponding shape is not as smooth as the one gained with terms of Fourier series. Therefore, the shapes defined with Fourier series are found to be more appropriate in the process of seeking the “worst” imperfection shape.

In the presented work an additional parameter, i.e. the maximum curvature of the plate, was introduced and analysed in order to influence the solution of the optimization method when seeking the worst imperfection shape. The main objective of the maximum curvature constraint is to influence the imperfection shape in a way that the final result is a realistic imperfection shape. In this step of the analysis engineering judgment is required to assess whether the imperfection shape is realistic or not. The maximum curvature limit was defined with a shift of the maximum amplitude from the mid span of the plate to $\frac{1}{4}$ of the plate span with maximum out-of-plane amplitude defined according to EN 1993-1-5. For very short plates the maximum curvature was limited to κ_{yield} .

One of the main observations, which should be further verified, is that the worst imperfection shape could be defined as deformed shape evaluated at the maximum LPF. Of course, this deformed shape should fulfil the following limits: out-of-plane imperfection amplitude and maximum curvature amplitude, otherwise the imperfection shape will significantly reduce the resistance of the element.

In many cases the 1st buckling mode is found as the worst imperfection, but this is not always the case. When searching for ultimate resistance of the structure it is a good practice to perform initial imperfection analysis with several buckling modes. But this might be time consuming; therefore, it would be enough to estimate the resistance with the 1st buckling mode and with deformation shape as it was found to be the “worst” initial imperfection.

Received on July 16, 2014

REFERENCES

1. KRISTANIČ, N., *Limit State Design Using Exact Sensitivity Analysis and Shape Optimization*, PhD Thesis, University of Ljubljana, Faculty of civil and geodetic engineering, Ljubljana, 2008.
2. KRISTANIČ, Niko, KORELC, Jože, *Optimization method for the determination of the most unfavorable imperfection of structures*, *Comput. Mech.*, **42**, 6, pp. 859–872, 2008.
3. *** CEN, *Eurocode 3: Design of steel structures. Part 1–5: Plated structural elements (EN 1993-1-5)*, European Committee for Standardisation, Brussels, 2006.
4. BEG, D., KUHLMANN, U., DAVAINÉ, L., BRAUN, B., *Design of Plated Structures. Eurocode 3: Design of Steel Structures. Part 1–5: Design of Plated Structures*, 1st edition, European Convention for Constructional Steelwork, Berlin, Ernst & Sohn, Brussels, 2010.
5. JOHANSSON, B., MAQUOI, R., SEDLACEK, G., MÜLLER, C., BEG, D., *Commentary and worked examples to EN 1993-1-5 Plated structural elements*, 1st edition, Office for Official Publications of the European Communities, Joint Research Centre European Commission, Luxembourg, 2007.
6. KORELC, J. *AceFEM, Mathematica finite element environment*, University of Ljubljana, Faculty of Civil and Geodetic Engineering, Ljubljana, 2010.
7. KUHLMANN, U., BEG, D., ZIZZA, A., SINUR, F., REJEC, K., *Tragverhalten von Blechen mit Längssteifen unter Interaktion von Biegemoment und Querkraft* (in German), Research Report, Universität, Institut für Konstruktion und Entwurf, Stuttgart, 2012.

